plated in triplicate into 12-well plates. At various time points cells were stained with crystal violet (Sigma) and the optical density at 590 nm was determined[15]. Values were normalized to the optical density at day 0 (20 h after plating). Phoenix producer cells were used to generate retroviral stocks as described[15]. For infection, subconfluent passage 1 MEF cultures were incubated at 37 °C with viral supernatant in the presence of 4 μg ml^{-1} polybrene (Sigma). After 6 h the viral supernatant was diluted 1:3 with complete medium and left on the cells for 42 h. Appropriate dilutions of viral supernatants were used such that 100% of MEFs were infected.

BrdU-incorporation assay and western blotting. MEFs were grown on coverslips and incubated for 4 h with 10 μM BrdU (Amersham). Cells were washed in PBS, fixed for 15 min at −20 °C in 5% acetic acid/95% ethanol and incubated in PBS. Fixed cells were incubated for 20 min in 2 M HCl/0.5% Triton-X100, for 30 min in blocking solution (5% fetal calf serum, 5% normal goat serum in PBS/0.02% Triton-X100), for 1 h with 1:10 diluted anti-BrdU monoclonal antibody (DAKO) in blocking solution, and overnight at 4 °C with 1:50 diluted fluorescein isothiocyanate (FITC)-conjugated goat anti-mouse antibody (Jackson Immuno Research Labs) and 4,-6-diamidino-2-phenylindole (DAPI) in blocking solution; this was followed by 3 washes for 5 min each in PBS/0.02% Triton-X100. Cells were embedded in Vectastain (Vector Labs) and the percentage of BrdU-labelled cells (FITC:DAPI ratio) was quantified using a fluorescence microscope. For protein analysis, cells were washed with PBS, scraped and lysed on ice in RIPA buffer (150 mM NaCl, 1% NP40, 0.1% SDS, 0.5% DOC, 50 mM Tris-HCl, pH 8.0, 2 mM EDTA, pH 8.0, 0.2 mM phenylmethylsulphonylfluoride (PMSF), 0.5 mM dithiothreitol (DTT)). Cleared lysates were assayed for protein concentration. Equal amounts of protein were separated on 12.5% SDS–PAGE and transferred to nitrocellulose. Western blot analysis was according to standard methods using enhanced chemiluminescence (Amersham). A list of antisera used is available on request.

Expression analysis. Total RNA was extracted using guanidinium thiocyanate, separated on 1.2% agarose, transferred to nitrocellulose and hybridized according to standard procedures with ^{32}P-labelled probes specific for exon 1α of mouse p16, for exon 1β of mouse p19^{Arf}, for mouse p15 or for rat glyceraldehyde-3-phosphate dehydrogenase (GAPDH). For semiquantitative reverse transcription with polymerase chain reaction (RT-PCR), first-strand complementary DNA was generated from 1 μg total RNA using Superscript II RT (Gibco) and oligo-dT primer according to the manufacturer's instructions. Primer sequences are available upon request. PCR reactions were performed on five-times serial dilutions of first-strand cDNA in 50 μl containing 1× Taq PCR buffer, 1.5 mM $MgCl_2$, 200 μM dNTPs, 0.5 μM of each of four primers, 1 μl of first-strand cDNA template and 1.25 units of Taq DNA Polymerase (Gibco), using 35 cycles of denaturation (94 °C, 1 min), annealing (60 °C, 45 s) and extension (72 °C, 2 min). Products were resolved on 2% NuSieve agarose gels.

Generation of *bmi-1*$^{-/-}$ *ink4a*$^{-/-}$ mice. *bmi-1*$^{+/-}$ FVB mice[4] and *ink4a*$^{+/-}$ mice on a mixed 129/Sv; C57BL/6 genetic background[24] were crossed to generate *bmi-1*$^{+/-}$ *ink4a*$^{+/-}$ mice, which were subsequently intercrossed to generate double-knockout offspring together with control littermates. Mice were genotyped routinely by PCR or Southern blot analysis of tail DNA.

Cell count and flow-cytometric analysis. Cell suspensions of lymphoid organs were prepared by mincing the tissue though an open filter chamber. Cell suspensions were depleted of erythrocytes and the number of nucleated cells was determined with a Casy-1 TT automated cell counter (Schäfe, Reutlingen, Germany). Flow cytometry with standard B- and T-cell differentiation was done nearly as described[10].

Histological analysis. Brains were fixed in 4% formaldehyde in PBS, paraffin-embedded and cut into 4-μm serial sagittal sections. Sections at different levels were stained with haematoxylin and eosin.

Received 10 September; accepted 12 November 1998.

1. van Lohuizen, M. *et al.* Identification of cooperating oncogenes in Eμ-*myc* transgenic mice by provirus tagging. *Cell* **65,** 735–752 (1991).
2. Haupt, Y., Alexander, W. S., Barri, G., Klinken, S. P. & Adams, J. M. Novel zinc finger gene implicated as myc collaborator by retrovirally accelerated lymphomagenesis in Eμ-myc transgenic mice. *Cell* **65,** 753–763 (1991).
3. van Lohuizen, M., Frasch, M., Wientjens, E. & Berns, A. Sequence similarity between the mammalian *Bmi-1* proto-oncogene and the *Drosophila* regulatory genes Psc and Su(z)2. *Nature* **353,** 353–355 (1991).
4. van der Lugt, N. M. T. *et al.* Posterior transformation, neurological abnormalities, and severe hematopoietic defects in mice with a targeted deletion of the *Bmi-1* proto-oncogene. *Genes Dev.* **8,** 757–769 (1994).
5. Alkema, M. J. *et al. MPc2*, a new murine homologue of the *Drosophila* Polycomb protein is a member of the mouse Polycomb transcriptional repressor complex. *J. Mol. Biol.* **273,** 993–1003 (1997).
6. Alkema, M. J., van der Lugt, N. M. T., Bobeldijk, R. C., Berns, A. & van Lohuizen, M. Transformation of axial skeleton due to overexpression of *Bmi-1* in transgenic mice. *Nature* **374,** 724–727 (1995).
7. Paro, R. Propagating memory of transcriptional states. *Trends Genet.* **11,** 295–298 (1995).
8. van Lohuizen, M. Functional analysis of mouse Polycomb-group genes. *Cell. Mol. Life Sci.* **54,** 71–79 (1998).
9. Gould, A. Functions of mammalian Polycomb group and trithorax group related genes. *Curr. Opin. Genet. Dev.* **7,** 488–494 (1997).
10. Alkema, M. J., Jacobs, H., van Lohuizen, M. & Berns, A. Perturbation of B and T cell development and predisposition to lymphomagenesis in Eμ-*Bmi1* transgenic mice require the Bmi1 RING finger. *Oncogene* **15,** 899–910 (1997).
11. Dimri, G. P. *et al.* A biomarker that identifies senescent human cells in culture and aging skin *in vivo*. *Proc. Natl Acad. Sci. USA* **92,** 9363–9367 (1995).
12. Hara, E. *et al.* Regulation of p16 CDKN2 expression and its implications for cell immortalisation and senescence. *Mol. Cell. Biol.* **16,** 859–867 (1996).
13. Alcorta, D. A. *et al.* Involvement of the cyclin-dependent kinase inhibitor p16 (INK4a) in replicative senescence of normal human fibroblasts. *Proc. Natl Acad. Sci. USA* **93,** 13742–13747 (1996).
14. Zindy, F., Quelle, D. E., Roussel, M. F. & Sherr, C. J. Expression of the p16ink4a tumour suppressor versus other ink4 family members during development and aging. *Oncogene* **15,** 203–211 (1997).
15. Serrano, M., Lin, A. W., McCurrach, M. E., Beach, D. & Lowe, S. W. Oncogenic ras provokes premature cell senescence associated with accumulation of p53 and p16ink4a. *Cell* **88,** 593–602 (1997).
16. Haber, D. A. Splicing into senescence: the curious case of p16 and p19^{Arf}. *Cell* **91,** 555–558 (1997).
17. Kamijo, T. *et al.* Tumour suppression at the mouse *ink4a* locus mediated by the alternative reading frame product p19^{Arf}. *Cell* **91,** 649–659 (1997).
18. Strutt, H., Cavalli, G. & Paro, R. Colocalisation of Polycomb protein and GAGA factor on regulatory elements responsible for the maintenance of homeotic gene expression. *EMBO J.* **12,** 3621–3632 (1997).
19. Cavalli, G. & Paro, R. The *Drosophila Fab-7* chromosomal element conveys epigenetic inheritance during mitosis and meiosis. *Cell* **93,** 505–518 (1998).
20. Pirotta, V. PcG complexes and chromatin silencing. *Curr. Opin. Genet. Dev.* **7,** 249–258 (1997).
21. Alkema, M. J. *et al.* Identification of Bmi1-interacting proteins as constituents of a multimeric mammalian Polycomb complex. *Genes Dev.* **11,** 226–240 (1997).
22. Gunster, M. J. *et al.* Identification and characterisation of interactions between the vertebrate Polycomb-group protein BMI1 and the human homologues of Polyhomeotic. *Mol. Cell. Biol.* **17,** 2326–2335 (1997).
23. Akasaka, T. *et al.* A role for *mel-18*, a *Polycomb* group-related vertebrate gene, during the anteroposterior specification of the axial skeleton. *Development* **122,** 1513–1522 (1996).
24. Serrano, M. *et al.* Role of the ink4a locus in tumour suppression and cell mortality. *Cell* **85,** 27–37 (1996).
25. Zindy, F. *et al.* Myc signalling via the ARF tumour suppressor regulates p53-dependent apoptosis and immortalisation. *Genes Dev.* **12,** 2424–2433 (1998).
26. de Stanchina, E. *et al.* E1A signalling to p53 involves the p19^{ARF} tumour suppressor. *Genes Dev.* **12,** 2434–2442 (1998).
27. Blyth, K. *et al.* Synergy between a human *c-myc* transgene and p53 null genotype in murine thymic lymphomas: contrasting effects of homozygous and heterozygous p53 loss. *Oncogene* **10,** 1717–1723 (1995).
28. Bodrug, S. E. *et al.* Cyclin D1 transgene impedes lymphocyte maturation and collaborates in lymphomagenesis with the *myc* gene. *EMBO J.* **13,** 2124–2130 (1994).
29. Mateyak, M. K., Obaya, A. J., Adachi, S. & Sedivy, J. M. Phenotypes of c-Myc-deficient Rat fibroblasts isolated by targeted homologous recombination. *Cell Growth Differ.* **8,** 1039–1048 (1997).
30. Hall, M. & Peters, G. Genetic alterations of cyclins, cyclin-dependent kinases and cdk inhibitors in human cancer. *Adv. Cancer Res.* **68,** 67–108 (1996).

Supplementary information is available on *Nature*'s World-Wide Web site (http://www.nature.com) or as paper copy from the London editorial office of *Nature*.

Acknowledgements. We thank G. Peters for p16 and p15 cDNA plasmids; H. Koseki and J. Deschamps for *mel-18*$^{-/-}$ embryos; T. Ide for the TiG-3 cells; J. Sedivy for c-*myc*$^{-/-}$ TGR-1 cells; S. Lowe, B. Amati, C. Sherr, M. Ewen, D. Peeper and R. Bernards for gifts of recombinant retroviral vectors; G. Nolan for providing phoenix eco- and amphotropic packaging cell lines and LZRS-IRES-EGFP retroviral vectors; N. van der Lugt for constructing the LZRS-*bmi-1*-IRES-EGFP retrovirus; E. de Pauw for telomere FISH analysis; and R. Bernards, A. Berns and W. Voncken for critically reading the manuscript J.J.L.J. and K.K. were supported by a grant of the Dutch Cancer Society (K.W.F.)

Correspondence and requests for materials should be addressed to M.v.L. (e-mail: lohuizen@nki.nl).

Robustness in bacterial chemotaxis

U. Alon*†, M. G. Surette‡, N. Barkai† & S. Leibler*†

*Departments of *Molecular Biology and †Physics, Princeton University, Princeton, New Jersey 08544, USA*

‡ Department of Microbiology and Infectious Diseases, Calgary, Alberta, Canada T2N 4N1

Networks of interacting proteins orchestrate the responses of living cells to a variety of external stimuli[1], but how sensitive is the functioning of these protein networks to variations in their biochemical parameters? One possibility is that to achieve appropriate function, the reaction rate constants and enzyme concentrations need to be adjusted in a precise manner, and any deviation from these 'fine-tuned' values ruins the network's performance. An alternative possibility is that key properties of

biochemical networks are robust[2]; that is, they are insensitive to the precise values of the biochemical parameters. Here we address this issue in experiments using chemotaxis of *Escherichia coli*, one of the best-characterized sensory systems[3,4]. We focus on how response and adaptation to attractant signals vary with systematic changes in the intracellular concentration of the components of the chemotaxis network. We find that some properties, such as steady-state behaviour and adaptation time, show strong variations in response to varying protein concentrations. In contrast, the precision of adaptation is robust and does not vary with the protein concentrations. This is consistent with a recently proposed molecular mechanism for exact adaptation, where robustness is a direct consequence of the network's architecture[2].

The *E. coli* chemotaxis system[3,4] has emerged as a prototype for understanding how processes at the network level arise from interactions between individual components[5,6]. The protein network responsible for chemotaxis has been characterized in detail[3,4] (Box 1). This sensory network governs the migration of bacteria towards chemical attractants and away from repellents by translating temporal changes in the level of chemical stimuli into a modulation of the cell's swimming direction. This is achieved by controlling the frequency of abrupt direction changes called tumbles. An important feature of chemotaxis is exact adaptation: a change in the concentration of a chemical stimulant induces a rapid change in the bacteria's tumbling frequency, which gradually adapts back precisely to its pre-stimulus value[7,8].

Once the components of a biochemical network are isolated and their interactions characterized, the mechanisms of the network's functioning can be addressed. Here, we focus on a distinct, complementary aspect, namely the sensitivity of the network's functioning to variations in its biochemical parameters. Specifically, we ask how sensitive exact adaptation in chemotaxis is to variations in the concentration of proteins in the network. Several theoretical proposals for the molecular mechanism of adaptation[5,9–11] required that the biochemical parameters of the chemotaxis network have to be fine-tuned to obtain exact adaptation. Deviations of the parameters from their fine-tuned values would result only in partial adaptation. In contrast, a recent analysis[2], based on a two-state model of chemoreceptors[3,12], proposed that exact adaptation is a robust property of chemotaxis. That is, the ability of the bacteria to adapt precisely would survive substantial variations in any of the biochemical parameters of the network.

To differentiate between the fine-tuned and robust scenarios, we systematically varied the concentrations of the chemotaxis-network proteins, and measured the resulting behaviour. Similar methods have been used in analyses of metabolic pathways[13]. The tumbling frequency, averaged over a population of swimming cells, was measured using a video microscopy image-analysis system[14]. Cells were stimulated by addition of a saturating amount of attractant (1 mM L-aspartate), and their behaviour was compared with that of unstimulated cells (Fig. 1). The cells responded to the attractant by suppressing tumbling. The tumbling frequency then increased as the cells adapted, with a characteristic adaptation time, reaching a new steady state. The adaptation precision, P, was defined as the ratio between the steady-state tumbling frequency of unstimulated and stimulated cells: wild-type cells showed exact adaptation[7,8,15] ($P = 0.98 \pm 0.05$, mean $\pm$ standard deviation (s.d.)). The same degree of adaptation precision was also found for other attractants and repellents (1 mM L-serine, 50 mM L-leucine, data not shown. Note, however, that a lower steady-state tumbling frequency was reported[15] in the presence of L-serine than in its absence under different buffer conditions).

One of the key proteins in the adaptation mechanism[3,4] is CheR, which is responsible for chemoreceptor methylation (Box 1). A strain deleted for *cheR* did not tumble and could not adapt (Fig. 2). Tumbling was restored by CheR expression under a *lac* promoter from a low-copy plasmid. Intracellular CheR concentrations were varied, over a range of ~100-fold, by induction with different amounts of isopropyl-β-D-thiogalactoside (IPTG), and the average CheR concentration was quantitated by immunoblots. The initial smooth swimming response of the cells to attractant (< 0.05 tumbles per s) was followed by adaptation. As CheR was varied between ~0.4 and 6 times wild-type concentration, the adaptation time, τ, varied more than 20-fold, from 23 ± 2 min to ~1 min (Fig. 2b). Similarly, the steady-state tumbling frequency, f, increased by about threefold. This is consistent qualitatively with model predictions[2] where $\tau \sim 1/[\mathrm{CheR}]$ and f increases with the intracellular CheR concentration [CheR]. The tumbling frequency saturated at about 0.75 tumbles per s at the highest concentration of CheR attained (about 50 times the wild-type concentration). Throughout these variations, adaptation remained precise to within experimental error (Fig. 2a).

Similar results were obtained when the concentrations of the

Box 1 Chemotaxis system of *E. coli*

Bacteria such as *E. coli* bias their swimming motion towards specific attractants and away from repellents[3,4]. Bacterial motion resembles a random walk, with periods of smooth swimming interrupted by brief tumbles that change the swimming direction[15]. Chemotaxis is achieved by modulation of the tumbling frequency. When moving up an attractant gradient, the bacteria encounter an attractant concentration that increases with time. In response, they tumble less frequency and thus tend to continue to move up the gradient. This process is mediated by a protein network[3,4] (see Box Figure below).

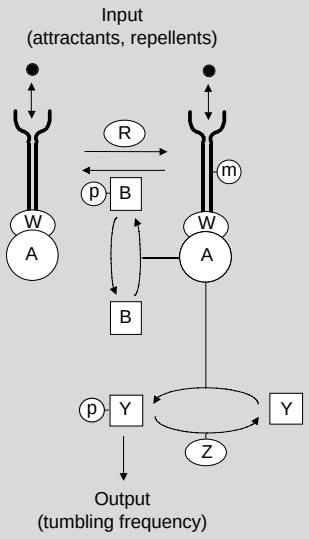

Information about the chemical environment is transduced into the cells by chemoreceptors, such as the aspartate receptor Tar, which span the membrane. The chemoreceptors form complexes inside the cells with the kinase CheA (A) and CheW (W). CheA phosphorylates itself and then transfers phosphoryl (P) groups to CheY (Y), a diffusible messenger protein. The phosphorylated form of CheY interacts with the flagellar motors to induce tumbles. The rate of CheY dephosphorylation is greatly enhanced by CheZ (Z). Binding of attractants to the receptors decreases the rate of CheY phosphorylation and tumbling is reduced. Adaptation is provided by changes in the level of methylation of the chemoreceptors: methylation increases the rate of CheY phosphorylation. A pair of enzymes, CheR (R) and CheB (B), add and remove methyl (m) groups. To adapt to an attractant, methylation of the receptors must rise to overcome the suppression of receptor activity caused by the attractant binding. CheA enhances the demethylating activity of CheB by phosphorylating CheB on its amino-terminal domain[20,21].

other proteins in the network were varied (Table 1). The steady-state tumbling frequency was affected by changes in concentration of these proteins, in qualitative agreement with previous studies[16–19]. For instance, an increase in the concentration of CheB, the receptor-demethylating enzyme (Box 1), caused a decrease in tumbling frequency and an increase in adaptation time. Loss of CheZ resulted in increased tumbling frequency, and the initial response to stimulation was a reduction in the tumbling frequency to about half of its adapted value, rather than to <0.05 tumbles per s as in the wild-type strain. This can be explained by the greatly reduced rate of CheY dephosphorylation in the absence of CheZ. Both tumbling frequency and adaptation time were modified upon simultaneous overexpression of the entire *meche* operon (encoding Tar, Tap, CheR, CheB, CheY and CheZ) from a plasmid. Strikingly, exact adaptation was observed for all of these perturbed networks (Table 1), which is consistent with the predictions of the robust-adaptation model[2].

To probe the mechanism for exact adaptation further, we used an activated mutant of CheB, CheBc, which can demethylate the receptors but lacks the domain phosphorylated by CheA[20,21]. This mutant lacks the feedback loop that was often thought to be responsible for exact adaptation[4,10,11]. In this feedback loop, the receptor-controlled kinase, CheA, phosphorylates CheB, increasing the demethylation of the receptors and thereby downregulating its own activity (Box 1). We find that cells deleted for *CheB* on the chromosome, but which express CheBc, show response and exact adaptation to attractant stimuli (Table 1). This seems to exclude CheB phosphorylation as the mechanism of exact adaptation, although it may be important in other aspects of chemotaxis[19,20]. In this context, the postulated molecular mechanism that leads to robust exact adaptation, analysed in ref. 2, is not based on the phosphorylation feedback loop. The crux of this mechanism is a different type of feedback in which CheB demethylates receptors only when they are in their active conformation[2,3,12].

The present results show that exact adaptation is maintained despite substantial variations in the network-protein concentrations. Why is adaptation precision a robust property, whereas properties such as adaptation time and steady-state behaviour are sensitive to variations in biochemical parameters? It is tempting to argue that properties that are critical to the functioning of the network are selected to be robust so that they can withstand natural variations. There is indeed some evidence that exact adaptation is important in the sensory process. It allows the system to compensate for the presence of continued stimulation, and to be ready to respond to further stimuli. Mutant bacteria that show only partial adaptation (strains deleted for both *cheR* and *cheB*[22–24]) are severely deficient in chemotaxis, as assayed by their net motion in attractant gradients[24,25], despite the fact that their steady-state tumbling frequency is close to that of the wild-type strain. In contrast, strains that have normal adaptation, but tumbling frequencies different from wild type, show chemotaxis ability that is comparable to the wild-type strain[26]. We confirmed this result using the present strains with varying CheR concentrations (data not shown). Furthermore, exact adaptation is found in other bacteria such as *Bacillus subtilis*[27] and *Rhodobacter sphaeroides*[28]. These results suggest that exact adaptation is critical for chemotaxis, whereas chemotaxis ability is not dependent on the precise value of the steady-state tumbling

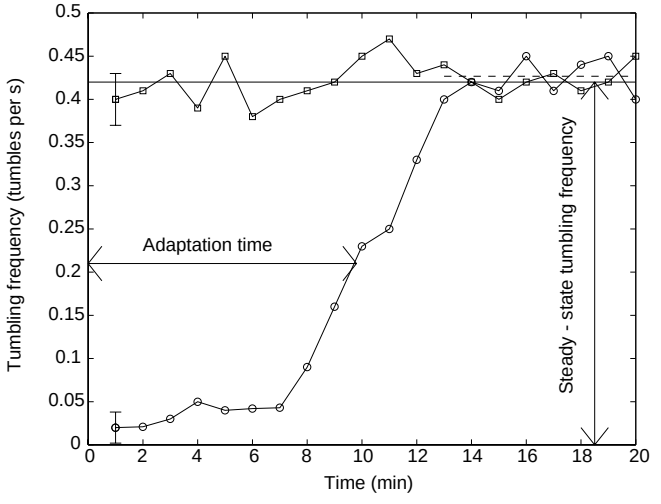

Figure 1 Tumbling frequency as a function of time for wild-type (RP437) cells. Circles: cells stimulated at time $t = 0$ by mixing with saturating attractant (1 mM L-aspartate). Squares: unstimulated cells (mock-mixed with chemotaxis buffer). Tumbling frequency was determined using computerized video tracking[14]. Each point represents data from 10 s motion of 100–400 cells. The adaptation time was defined as the time where the tumbling frequency of stimulated cells rises to halfway between its earliest measured value and its steady-state value. Precision of adaptation was defined as the ratio between the steady-state tumbling frequency of unstimulated cells (full horizontal line) and stimulated cells (dashed horizontal line).

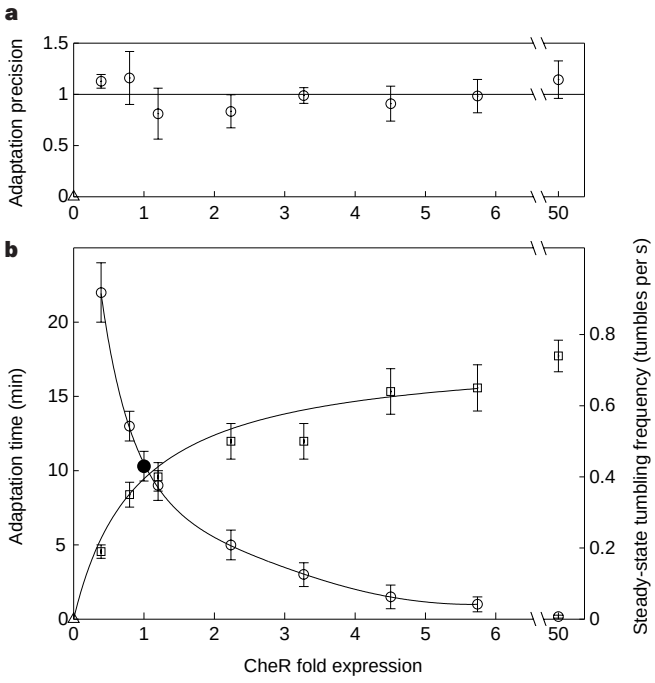

Figure 2 Chemotaxis behaviour of cells with varying intracellular concentration of the protein CheR. CheR was expressed from the plasmid pUA4 with varying levels of IPTG induction in a strain deleted for *cheR* (RP4968). **a**, Precision of adaptation, defined as the ratio between the steady-state tumbling frequency of unstimulated cells and cells stimulated with 1 mM L-aspartate. A precision of 1.0 corresponds to exact adaptation. Cells lacking CheR (RP4968 with the control vector pHSG575, triangle) did not respond to attractants, but showed a persistent response of about 0.6 tumbles per s to repellent (50 mM L-leucine). **b**, Average steady-state tumbling frequency of unstimulated cells (open squares, right scale), and average adaptation time to a step-like stimulation with 1 mM L-aspartate (open circles, left scale). Solid circle, wild-type strain (RP437 + pHSG575). Triangle, tumbling frequency of RP4968 + pHSG575. Lines are guides to the eye. Relative CheR expression was measured by immunoblots. 'Wild-type' CheR concentration was defined as the induction level where the adaptation time was equal to that of RP437 + pHSG575. Immunoblots also showed that the level of other chemotaxis proteins (CheB and CheY) did not vary measurably with CheR expression. Errors in relative CheR level are estimated to be under 30%. Mean and standard deviation of triplicate experiments are shown.

Table 1 Effect of variation in chemotaxis protein levels on behaviour

Protein varied	Fold expression	Strain background	Steady-state tumbling frequency (s^{-1})	Adaptation time (min)	Precision of adaptation
Wild type	1.0	Wild type (RP437)	0.44 ± 0.03	10 ± 1	0.98 ± 0.05
CheB*	0.4 ± 0.1	ΔcheB (RP4972)	0.66 ± 0.05	7 ± 1	0.98 ± 0.12
CheB*	12 ± 3	ΔcheB (RP4972)	0.14 ± 0.02	15 ± 1	1.09 ± 0.11
CheBc†	~1‖	ΔcheB (RP4972)	0.74 ± 0.06	9 ± 2	0.90 ± 0.13
CheY‡	0.2 ± 0.1	ΔcheY,Z (RP5231)	0.24 ± 0.04	11 ± 3	1.04 ± 0.08
CheZ	0	ΔcheZ (RP1616)	1.6 ± 0.1	10 ± 2	1.1 ± 0.14
Tar, Tap, CheR,B,Y,Z§	5 ± 2¶	Wild-type (RP437)	0.30 ± 0.06	3 ± 1	1.04 ± 0.07

Cells were stimulated with 1 mM L-aspartate. Behavioural results are mean and standard deviation of triplicate experiments. Fold expression is relative to RP437, shown as mean and standard deviation of four independent immunoblot determinations using affinity-purified polyclonal antibodies.
* Plasmid pUA3.
† Plasmid pME304 (ref. 21).
‡ Plasmid pLC576 (ref. 14).
§ Plasmid pCR73 (ref. 18).
‖ CheBc fold expression estimated against wild-type CheB in RP437.
¶ Determined using antibodies against CheR and CheB.

frequency and the adaptation time. Exact adaptation might also be a 'side effect' of the mechanism for a different, critical aspect of chemotaxis (for example, the amplification or gain of the system[6,22]), and as such could be selected as a robust property.

The experimental approach presented here can be generalized to other biochemical or genetic networks. For a given network, those functional properties that are robust, and those that are sensitive with respect to parameter variations could be classified. It would then be interesting to see whether any 'design principles' connected with robustness, perhaps analogous to those used in engineering, emerge from such systematic studies. □

Methods

Bacterial strains and plasmids. All strains were derivatives of *E. coli* K12 strain RP437 [*thr leu his metF eda rpsL thi ara lacY xyl tonA tsx*], which is wild type for chemotaxis[16]. pUA4 was constructed by subcloning an *Xba*I–*Hin*dIII fragment of pME1 (ref. 29) containing *cheR* from *S. typhimurium* and the *Eco*RI-*Sba*I fragment of pUC054 (ref. 30) containing *lacI*^{q} into the low-copy vector pHSG575 (ref. 14). An *Eco*RI–*Hin*dIII fragment of pME30 (ref. 29) containing *cheB* from *S. typhimurium* was subcloned into pBAD18 (ref. 14) to yield pUA3. Similar results were obtained with cells expressing *E. coli* CheR and CheB from the plasmids p43:cheR (ref. 18) and p43:cheB (ref. 18). Other plasmids are listed in Table 1.

Behavioural assays. Cultures, grown overnight at 30 °C in Tryptone broth[14] with selective antibiotics, were diluted 1:50 into 20 ml Tryptone broth in 125-ml flasks, shaken at 200 r.p.m. at 30 °C, induced after 2 h and collected at $A_{600} = 0.5$ (5×10^8 cells ml^{-1}). Cells were washed twice at 800*g* into chemotaxis buffer[14] (7.6 mM $(NH_4)_2$, 2 mM $MgSO_4$, 20 μM $FeSO_4$, 0.1 mM EDTA, 0.1 mM L-methionine, 60 mM potassium phosphate, pH 6.8), and incubated for 15 min at room temperature. A sample (10 μl) of cell suspension was stimulated by mixing with 10 μl of 2 mM L-aspartate in chemotaxis buffer, or mock stimulated by mixing with 10 μl chemotaxis buffer. Cells (0.5 μl) were then placed in the centre of a circle inscribed with a china marker on a vinyl slide and covered by a vinyl coverslip (Fisher), creating a several-micron-thick fluid layer. To prevent cell adhesion to the surfaces, slides and coverslips were precoated by dipping in a solution of 0.1% bovine serum albumin (BSA) (>99% purity; Sigma) in chemotaxis buffer followed by a brief wash in distilled water. Bacteria were observed with dark-field video microscopy (Nikon Optiphot-2; field of view spanned 220 μm), and average tumbling frequency was determined by computerized image analysis as previously described[14]. The behaviour with 1 mM L-aspartate stimuli was indistinguishable from that observed in control experiments with 0.5 mM or 10 mM L-aspartate stimuli. Chemotaxis ability was assayed on soft agar plates (Tryptone broth + 0.3% agar) at 30 °C[17].

Protein quantitation. Cultures, grown as for the behavioural assays, were subjected to SDS–polyacrylamide gel electrophoresis and western blot analysis as described[14]. To determine relative expression in strains A and B, where B has a higher copy number per cell of the protein assayed, lysates of strain B were diluted with various amounts of PS2002 (ref. 14) lysate (an RP437 derivative deleted for *Tar*, *Tap* and all of the *che* genes) and compared with standards of strain A (equal total protein in each lane). The diluted strain intensities bracketed the standard intensity.

Received 13 October; accepted 27 November 1998.

1. Bray, D. Protein molecules as computational elements in living cells. *Nature* **376,** 307–312 (1995).
2. Barkai, N. & Leibler, S. Robustness in simple biochemical networks. *Nature* **387,** 913–917 (1997).
3. Stock, J. B. & Surette, M. G. in *Escherichia coli and Salmonella, Cellular and Molecular Biology* (ed. Neidhardt, F. C.) 1103–1129 (ASM Press, Washington, 1996).
4. Falke, J. J., Bass, R. B., Butler, S. L., Chervitz, S. A. & Danielson, M. A. The two-component signaling pathway of bacterial chemotaxis: a molecular view of signal transduction by receptors, kinases, and adaptation enzymes. *Annu. Rev. Cell Dev. Biol.* **13,** 457–512 (1997).
5. Bray, D., Bourret, R. B. & Simon, M. I. Computer simulation of the phosphorylation cascade controlling bacterial chemotaxis. *Mol. Biol. Cell* **5,** 469–482 (1993).
6. Bray, D., Levin, M. D. & Morton-Firth, C. J. Receptor clustering as a cellular mechanism to control sensitivity. *Nature* **393,** 85–88 (1998).
7. Macnab, R. M. & Koshland, D. E. The gradient sensing mechanism in bacterial chemotaxis. *Proc. Natl Acad. Sci. USA* **69,** 2509–2512 (1972).
8. Berg, H. C. & Tedesco, P. Transient response to chemotaxis stimuli in *Escherichia coli*. *Proc. Natl Acad. Sci. USA* **72,** 3235–3239 (1975).
9. Segel, L. A., Goldbeter, A., Devrotes, P. N. & Knox, B. E. A mechanism for exact sensory adaptation based on receptor modification. *J. Theor. Biol.* **120,** 151–179 (1986).
10. Hauri, D. C. & Ross, J. A. A model of excitation and adaption in bacterial chemotaxis. *Biophys. J.* **68,** 708–722 (1995).
11. Spiro, P. A., Parkinson, J. S. & Othmer, H. G. A model of excitation and adaptation in bacterial chemotaxis. *Proc. Natl Acad. Sci. USA* **94,** 7263–7268 (1997).
12. Asakura, S. & Honda, H. Two-state model for bacterial chemoreceptor proteins. *J. Mol. Biol.* **176,** 349–367 (1984).
13. Fell, D. *Understanding the Control of Metabolism* (Portland Press, London, 1997).
14. Alon, U. *et al.* Response regulator output in bacterial chemotaxis. *EMBO J.* **17,** 4238–4248 (1998).
15. Berg, H. C. & Brown, D. A. Chemotaxis in *Escherichia coli* analysed by three-dimensional tracking. *Nature* **239,** 500–504 (1972).
16. Parkinson, J. S. & Houts, S. Isolation and behavior of *Escherichia coli* deletion mutants lacking chemotaxis function. *J. Bacteriol.* **151,** 106–113 (1982).
17. Wolfe, A. J., Conley, P. M., Kramer, T. J. & Berg, H. C. Reconstitution of signaling in bacterial chemotaxis. *J. Bacteriol.* **169,** 1878–1885 (1987).
18. Russel, C. B., Stewart, R. C. & Dahlquist, F. W. Control of transducer methylation levels in *Escherichia coli*: investigation of components essential for modulation of methylation and demethylation reactions. *J. Bacteriol.* **171,** 3609–3618 (1989).
19. Levin, M., Morton-Firth, C., Abouhamad, W., Bourret, R. & Bray, D. Origins of individual swimming behavior in bacteria. *Biophys. J.* **74,** 175–181 (1998).
20. Stewart, R. C., Russel, C. B., Roth, A. F. & Dahlquist, F. W. Interaction of CheB with chemotaxis signal transduction components in *Escherichia coli*: modulation of the methylesterase activity and effects on cell swimming behavior. *Cold Spring Harb. Symp. Quant. Biol.* **LIII,** 27–40 (1988).
21. Lupas, A. & Stock, J. B. Phosphorylation of an N-terminus regulatory domain activates the CheB methylesterase in bacterial chemotaxis. *J. Biol. Chem.* **264,** 17337–17342 (1989).
22. Segall, J. E., Block, S. M. & Berg, H. C. Temporal comparisons in bacterial chemotaxis. *Proc. Natl Acad. Sci. USA* **83,** 8987–8991 (1986).
23. Stock, J., Kersulis, G. & Koshland, D. E. Neither methylating nor demethylating enzymes are required for bacterial chemotaxis. *Cell* **42,** 683–690 (1985).
24. Weis, R. M. & Koshland, D. E. Reversible methylation is essential for normal chemotaxis in *Escherichia coli* in gradients of aspartic acid. *Proc. Natl Acad. Sci. USA* **86,** 83–87 (1988).
25. Berg, H. & Turner, L. Chemotaxis of bacteria in glass capillary arrays. *Biophys. J.* **58,** 919–930 (1990).
26. Weis, R. M. & Koshland, D. E. Chemotaxis in *Escherichia coli* proceeds efficiently from different initial tumble frequencies. *J. Bacteriol.* **172,** 1099–1105 (1990).
27. Kirsch, M. L. *et al.* Chemotactic methyltransferase promotes adaptation to repellents in *Bacillus subtilis*. *J. Biol. Chem.* **268,** 25350–25356 (1993).
28. Grishanin, R. N., Gauden, D. E. & Armitage, J. P. Photoresponses in *Rhodobacter sphaeroides*: role of photosynthetic electron transport. *J. Bacteriol.* **179,** 24–30 (1997).
29. Simms, A. S., Keane, M. G. & Stock, J. B. Multiple forms of the CheB methyltransferase in bacterial chemosensing. *J. Biol. Chem.* **260,** 10161–10168 (1985).
30. Surette, M. G. & Stock, J. B. Role of α-helical coiled-coil interactions in receptor dimerization, signaling and adaptation during bacterial chemotaxis. *J. Biol. Chem.* **271,** 17966–17973 (1996).

Acknowledgements. We thank S. Block, H. Berg, P. Cluzel, M. Elowitz, L. Hartwell, M. Levit, A. Murray, M. Simon, J. Staropoli, R. Stewart and J. Stock for discussions, and J. Parkinson, F. Dahlquist and J. Stock for providing strains, antibodies and plasmids. N.B. is a Dicke fellow. U.A. is a Rothchild and a Markee fellow; he dedicates this work to the memory of I. Bentov.

Correspondence and requests for materials should be addressed to S.L. (e-mail: leibler@princeton.edu).